

**ENHANCING PHOTOCATALYTIC ABILITY OF  
TITANIUM DIOXIDE THROUGH  
INCORPORATION OF MIL-53(Fe) TOWARDS  
DEGRADATION OF METHYL ORANGE  
AND METHYLENE BLUE**



**NURUL Wafa Binti Othman**

**UMS**  
UNIVERSITI MALAYSIA SABAH

**FACULTY OF SCIENCE AND NATURAL  
RESOURCES  
UNIVERSITI MALAYSIA SABAH  
2017**

**ENHANCING PHOTOCATALYTIC ACTIVITY OF  
TITANIUM DIOXIDE THROUGH  
INCORPORATION OF MIL-53(Fe) TOWARDS  
DEGRADATION OF METHYL ORANGE  
AND METHYLENE BLUE**

**NURUL WAFA BINTI OTHMAN**



**A THESIS SUBMITTED IN FULFILLMENT  
WITH THE REQUIREMENT FOR THE DEGREE  
OF MASTER OF SCIENCE**

**FACULTY OF SCIENCE AND NATURAL  
RESOURCES  
UNIVERSITI MALAYSIA SABAH  
2017**

## **DECLARATION**

I hereby declare that the material in this thesis is my own except for quotations, excerpts, equations, summaries and references, which have been duly acknowledged.

1<sup>st</sup> November 2016

---

Nurul Wafa Binti Othman

MS1311007T



**UMS**  
UNIVERSITI MALAYSIA SABAH

## CERTIFICATION

NAME : **NURUL Wafa Binti Othman**

MATRIC NO. : **MS1311007T**

TITLE : **ENHANCING PHOTOCATALYTIC ACTIVITY OF TITANIUM  
DIOXIDE THROUGH INCORPORATION OF MIL-53(FE)  
TOWARDS DEGRADATION OF METHYL ORANGE (MO) AND  
METHYLENE BLUE (MB)**

DEGREE : **MASTER OF SCIENCE (INDUSTRIAL CHEMISTRY)**

DATE OF VIVA : **28 APRIL 2017**



CERTIFIED BY  
**UTMS**  
UNIVERSITI MALAYSIA SABAH

SIGNATURE

---

## **ACKNOWLEDGEMENTS**

It would not have been possible to completely write this thesis without the help and support from all the kind people around me. I am very grateful to be able to work and learn many useful knowledge and skills throughout my master project. I would like to take this opportunity to express my sincere appreciation and gratitude to my supervisor, Dr. Moh Pak Yan, who was willing to guide me during my master research journey, enhancing my critical thinking skills, his continuous support, his patience, motivation, enthusiasm and immense knowledge. Next, I would like to express my gratitude to Faculty of Science and Human Resources and Water Research Unit that provides instruments and equipments that aid me during my research. Not forgetting to lab assistant Mr. Jerry Alexander for his cooperation in providing me all the apparatus needed in my research, Mr. Abdul Rahim of XRD laboratory and Mdm. Marlenny of SEM laboratory for their patience with me.

I would also like to thanks the Ministry of Education for the provision of grant: ERGS0032-STG-1-2013. My sincere thanks to my colleagues Suzanna Wong, Nguang Sing Yew, Hasmira Radde, Cheong Von Fei and Michelle whom worked closely together with me in completing my research study, sharing knowledge and ideas to solve problems and cooperation in many ways.

Last but not least, I would love to express my deepest gratitude and love towards my parents, Othman bin Abdul Hamid and Rusnah binti Dahalan, my husband, Umair bin Muhammad Tahar, my siblings for their continuous love and support, encouraging me to complete my master research study. Once again, I am grateful for everything and hope for the best in the future.

Nurul Wafa Binti Othman

1<sup>st</sup> November 2016

## ABSTRACT

MIL-53(Fe) is an iron(III) carboxylate compound fall under the subclass of metal-organic frameworks (MOFs). This compound was incorporated to  $\text{TiO}_2$ , a non-toxic and highly efficient semiconductor for photocatalysis application. MIL-53(Fe) was synthesized by reflux method for 3 hours. The obtained MIL-53(Fe) powder was dispersed in ethanol and water mixture, sonicated and injected with a titanium(IV) butoxide. The mixture was then further heated in Teflon-lined autoclave to produce MIL-53(Fe)/ $\text{TiO}_2$ . To produce MIL-53(Fe) derived  $\text{Fe}_2\text{O}_3/\text{TiO}_2$  composite, the powder was calcined at 500 °C. XRD pattern confirmed the obtained powder corresponds to the MIL-53(Fe)/ $\text{TiO}_2$  with characteristic feature of an anatase and MIL-53(Fe), while the XRD pattern of the calcined MIL-53(Fe)/ $\text{TiO}_2$  powder suggested that the derived material were  $\text{Fe}_2\text{O}_3/\text{TiO}_2$  composite. EDX data proved that there was MIL-53(Fe) material incorporated to the  $\text{TiO}_2$ . Scanning Electron Microscope (SEM) image of MIL-53(Fe) showed a triangular prism-shaped with particle size in the range of 0.2 to 0.25  $\mu\text{m}$ . A spherical morphology were observed on MIL-53(Fe)/ $\text{TiO}_2$  and MIL-53(Fe) derived  $\text{Fe}_2\text{O}_3/\text{TiO}_2$  composites with the particle size in the range of 0.73 to 0.94  $\mu\text{m}$  and 0.61 to 0.81  $\mu\text{m}$  respectively. The photocatalytic activity of photocatalyst MIL-53(Fe)/ $\text{TiO}_2$ , MIL-53(Fe) derived  $\text{Fe}_2\text{O}_3/\text{TiO}_2$  and a control sample of  $\text{TiO}_2$  nano powder were evaluated towards methyl orange (MO) and methylene blue (MB) dye in water under UV-vis light irradiation at different time interval for 6 hours time. The results revealed that both MIL-53(Fe)/ $\text{TiO}_2$  and MIL-53(Fe) derived  $\text{Fe}_2\text{O}_3/\text{TiO}_2$  materials exhibit better photocatalytic activity compared to the bare  $\text{TiO}_2$ . MIL-53(Fe)/ $\text{TiO}_2$  has slightly increased the photocatalytic performance of  $\text{TiO}_2$  for about 6% towards MO and 11% towards MB while MIL-53(Fe) derived  $\text{Fe}_2\text{O}_3/\text{TiO}_2$  has successfully increased the photocatalytic performance of bare  $\text{TiO}_2$  for about 75% in MO and 30% in MB dye. The results obtained show that, the MIL-53(Fe) derived  $\text{Fe}_2\text{O}_3/\text{TiO}_2$  has good photocatalytic degradation efficiency compared to MIL-53(Fe)/ $\text{TiO}_2$ . This implies that MIL-53(Fe) derived  $\text{Fe}_2\text{O}_3/\text{TiO}_2$  is a potential material for environmental remediation such as water purification and air purification.

## **ABSTRAK**

### **PENINGKATAN KEUPAYAAN FOTOPEMANGKINAN TITANIUM DIOKSIDA MELALUI PERGABUNGAN MIL-53(Fe) KE ARAH DEGRADASI METIL JINGGA DAN METILEN BIRU**

MIL-53(Fe) adalah merupakan sebatian karboksilat besi(III) di bawah pengkelasan rangka logam organik. Sebatian ini telah digabungkan ke dalam titanium dioksida, semikonduktor yang tidak toksik dan cekap dalam aplikasi fotopemangkinan. MIL-53(Fe) disintesis menggunakan kaedah refluks selama 3 jam. Serbuk MIL-53(Fe) yang diperoleh di suraikan, di sonikasi, dan disuntik dengan titanium(IV) butoksida. Campuran tersebut kemudiannya dipanaskan di dalam autoklaf Teflon untuk menghasilkan MIL-53(Fe)/TiO<sub>2</sub>. Manakala untuk menghasilkan komposit Fe<sub>2</sub>O<sub>3</sub>/TiO<sub>2</sub> terbitan MIL-53(Fe), serbuk tersebut telah dikalsinasi pada suhu 500 °C. Corak XRD membuktikan serbuk yang diperoleh merupakan MIL-53(Fe)/TiO<sub>2</sub> dengan ciri anatasa manakala corak XRD MIL-53(Fe)/TiO<sub>2</sub> yang dikalsinasi menunjukkan bahawa bahan terbitan tersebut merupakan komposit Fe<sub>2</sub>O<sub>3</sub>/TiO<sub>2</sub>. Data dari spektroskopi tenaga serakan sinar-x membuktikan bahawa MIL-53(Fe) bergabung pada TiO<sub>2</sub>. Gambar SEM MIL-53(Fe) menunjukkan bentuk prisma segi tiga dengan saiz zarah pada kadar 0.2 kepada 0.25 µm. Morfologi sfera dapat dilihat pada komposit MIL-53(Fe)/TiO<sub>2</sub> dan Fe<sub>2</sub>O<sub>3</sub>/TiO<sub>2</sub> terbitan MIL-53(Fe) masing-masing dengan kadar saiz antara 0.73 kepada 0.94 µm dan 0.61 kepada 0.81 µm. Aktiviti pemangkinanfoto MIL-53(Fe)/TiO<sub>2</sub>, Fe<sub>2</sub>O<sub>3</sub>/TiO<sub>2</sub> terbitan MIL-53(Fe) dan sampel serbuk TiO<sub>2</sub> telah dinilai ke atas larutan pewarna metil jingga dan metilen biru dibawah pancaran cahaya UV pada selang masa yang berbeza selama 6 jam. Keputusan tersebut menunjukkan bahawa kedua-dua pemangkin foto MIL-53(Fe)/TiO<sub>2</sub> dan Fe<sub>2</sub>O<sub>3</sub>/TiO<sub>2</sub> terbitan MIL-53(Fe) mempamerkan aktiviti pemangkinan foto yang lebih baik jika dibandingkan dengan TiO<sub>2</sub>. MIL-53(Fe)/TiO<sub>2</sub> telah meningkatkan prestasi fotopemangkinan TiO<sub>2</sub> pada kadar 6% di dalam MO dan 11% pada MB manakala Fe<sub>2</sub>O<sub>3</sub>/TiO<sub>2</sub> terbitan MIL-53(Fe) telah berjaya meningkatkan prestasi fotopemangkinan TiO<sub>2</sub> pada kadar 75% di dalam MO dan 30% pada MB. Daripada keputusan yang diperoleh, Fe<sub>2</sub>O<sub>3</sub>/TiO<sub>2</sub> terbitan MIL-53(Fe) menunjukkan keberkesanan degradasi fotopemangkinan yang lebih baik berbanding MIL-53(Fe)/TiO<sub>2</sub>. Ini menunjukkan bahawa Fe<sub>2</sub>O<sub>3</sub>/TiO<sub>2</sub> terbitan MIL-53(Fe) adalah bahan yang berpotensi untuk pe/mulihan alam sekitar seperti pembersihan air dan udara.

# TABLE OF CONTENTS

	Page
<b>TITLE</b>	i
<b>DECLARATION</b>	ii
<b>CERTIFICATION</b>	iii
<b>ACKNOWLEDGEMENTS</b>	iv
<b>ABSTRACT</b>	v
<b>ABSTRAK</b>	vi
<b>TABLE OF CONTENTS</b>	vii
<b>LIST OF TABLES</b>	x
<b>LIST OF FIGURES</b>	xi
<b>LIST OF SYMBOLS AND ABBREVIATIONS</b>	xiv
<b>LIST OF APPENDICES</b>	xv
<b>CHAPTER 1: INTRODUCTION</b>	1
1.1 Photocatalytic Degradation of Organic Pollutants by Titanium	1
1.2 Problems of TiO <sub>2</sub> as Photocatalyst	2
1.3 Modification of TiO <sub>2</sub> with Metal-Organic Frameworks (MOFs)	3
1.4 Objectives	5
1.5 Scope of Study	5
<b>CHAPTER 2: LITERATURE REVIEW</b>	7
2.1 Advanced Oxidation Processes (AOP)	7
2.1.1 Titanium Dioxide (TiO <sub>2</sub> ) Assisted Heterogeneous Photocatalysis	10
2.2 Titanium Dioxide (TiO <sub>2</sub> )	12
2.2.1 Structure and Properties of TiO <sub>2</sub>	13
2.2.2 Synthesis of TiO <sub>2</sub>	15
2.2.3 Applications of TiO <sub>2</sub>	17
2.3 Metal-organic Frameworks (MOFs)	21
2.3.1 Introduction to Metal-organic Frameworks	22
2.3.2 Structure and Properties of MOFs	23
2.3.3 Synthesis of MOFs	25
2.3.4 Application of MOFs	29



	Page
2.3.5 MIL-53(Fe)	30
2.3.6 MOF-Derived Metal Oxide	32
2.4 Photocatalytic Degradation of Dyes	34
2.4.1 Dyes	34
2.4.2 Kinetics of Photocatalytic Degradation of Dyes	35
<b>CHAPTER 3: METHODOLOGY</b>	<b>36</b>
3.1 Chemicals and Instrumentation	36
3.1.1 Chemicals	36
3.1.2 Instruments	37
3.2 Preparation of MIL-53(Fe)/TiO <sub>2</sub> and MIL-53(Fe) derived Fe <sub>2</sub> O <sub>3</sub> /TiO <sub>2</sub> Photocatalysts	38
3.2.1 Synthesis of MIL-53(Fe) powder	37
3.2.2 Synthesis of TiO <sub>2</sub> powder	38
3.2.3 Synthesis of MIL-53(Fe)/TiO <sub>2</sub> and MIL-53(Fe) derived Fe <sub>2</sub> O <sub>3</sub> /TiO <sub>2</sub> photocatalysts	40
3.3 Characterization of MIL-53(Fe), TiO <sub>2</sub> , MIL-53(Fe)/TiO <sub>2</sub> and MIL-53(Fe) derived Fe <sub>2</sub> O <sub>3</sub> /TiO <sub>2</sub> Photocatalysts	41
3.3.1 Confirmation of materials by using XRD	40
3.3.2 Morphology of materials analysis by using SEM-EDX	41
3.4 Photocatalytic Degradation of Organic Dyes by MIL-53(Fe)/TiO <sub>2</sub> and MIL-53(Fe) derived Fe <sub>2</sub> O <sub>3</sub> /TiO <sub>2</sub> Photocatalysts	44
3.4.1 Preparation of MB solution	43
3.4.2 Preparation of MO solution	43
3.4.3 Setup of batch photoreactor	43
3.4.4 Photocatalytic degradation of organic dyes by MIL-53(Fe)/TiO <sub>2</sub> and MIL-53(Fe) derived Fe <sub>2</sub> O <sub>3</sub> /TiO <sub>2</sub> photocatalyst	45
<b>CHAPTER 4: PREPARATION AND CHARACTERIZATION OF MIL-53(Fe)/TiO<sub>2</sub> AND MIL-53(Fe) DERIVED Fe<sub>2</sub>O<sub>3</sub>/TiO<sub>2</sub></b>	<b>49</b>
4.1 Synthesis of MIL-53(Fe) and TiO <sub>2</sub>	47
4.1.1 MIL-53(Fe)	47
4.1.2 TiO <sub>2</sub>	48
4.2 Synthesis of MIL-53(Fe)/TiO <sub>2</sub> and MIL-53(Fe) Derived Fe <sub>2</sub> O <sub>3</sub> /TiO <sub>2</sub> Photocatalyst	51

	Page
4.2.1 Phase Identification of MIL-53(Fe), TiO <sub>2</sub> , MIL-53(Fe)/TiO <sub>2</sub> and MIL-53(Fe) derived Fe <sub>2</sub> O <sub>3</sub> /TiO <sub>2</sub> Photocatalyst	53
4.2.2 EDX Analysis of MIL-53(Fe), TiO <sub>2</sub> , MIL-53(Fe)/TiO <sub>2</sub> and MIL-53(Fe) derived Fe <sub>2</sub> O <sub>3</sub> /TiO <sub>2</sub> Photocatalyst	56
4.2.3 Surface Morphology of MIL-53(Fe), TiO <sub>2</sub> and MIL-53(Fe)/TiO <sub>2</sub> Photocatalyst	60
<b>CHAPTER 5: PHOTOCATALYTIC ACTIVITY OF MIL-53(Fe)/TiO<sub>2</sub> AND MIL-53(Fe) DERIVED Fe<sub>2</sub>O<sub>3</sub>/TiO<sub>2</sub></b>	<b>64</b>
5.1 Introduction	61
5.1.1 Effect of MIL-53(Fe) to TiO <sub>2</sub> ratio	61
5.1.2 Effect of MIL-53(Fe)/TiO <sub>2</sub> and MIL-53(Fe) derived Fe <sub>2</sub> O <sub>3</sub> /TiO <sub>2</sub> amount	69
5.1.3 Efficiency of material in different type of dye solutions	69
5.1.4 Effect of Initial Hydrogen Peroxide Concentrations Towards Reactivity of MIL-53(Fe)/TiO <sub>2</sub>	75
5.2 Kinetics Study of MO and MB Dye Degradation	76
5.3 Photocatalytic Mechanism of MIL-53(Fe)/TiO <sub>2</sub> and MIL-53(Fe) derived Fe <sub>2</sub> O <sub>3</sub> /TiO <sub>2</sub>	83
<b>CHAPTER 6: CONCLUSION AND FUTURE RECOMMENDATIONS</b>	<b>84</b>
6.1 Conclusion	84
6.2 Future Recommendations	85
<b>REFERENCES</b>	<b>86</b>
<b>APPENDICES</b>	<b>101</b>

## LIST OF TABLES

	Page
Table 2.1: Comparison of relative oxidation power of some oxidizing species.	8
Table 2.2: Types and classification of advanced oxidation processes.	10
Table 2.3: Crystal structure data of rutile, anatase and brookite.	15
Table 3.1: List of chemicals.	36
Table 3.2: List of instruments.	37
Table 3.3: Photocatalytic degradation of MO and MB solutions by different type of catalysts, photocatalyst amount, amount of MIL-53(Fe) incorporated into TiO <sub>2</sub> and effect of H <sub>2</sub> O <sub>2</sub> .	46
Table 5.1: Summary for degradation efficiency of different ratio of MIL-53(Fe) to TiO <sub>2</sub> ratio of MIL-53(Fe)/TiO <sub>2</sub> and MIL-53(Fe) derived Fe <sub>2</sub> O <sub>3</sub> /TiO <sub>2</sub> in photocatalytic degradation of MO and MB in water after 6 hours.	66
Table 5.2: Summary for degradation efficiency of different amount of MIL-53(Fe)/TiO <sub>2</sub> of MIL-53(Fe)/TiO <sub>2</sub> and MIL-53(Fe) derived Fe <sub>2</sub> O <sub>3</sub> /TiO <sub>2</sub> in photocatalytic degradation of mo and mb in water after 6 hours.	69
Table 5.3: Summary for degradation efficiency of MIL-53(Fe)/TiO <sub>2</sub> and MIL-53(Fe) derived Fe <sub>2</sub> O <sub>3</sub> /TiO <sub>2</sub> in photocatalytic degradation of MO and MB in water after 6 hours.	72
Table 5.4: Summary for degradation efficiency with addition of different concentration of H <sub>2</sub> O <sub>2</sub> in MIL-53(Fe)/TiO <sub>2</sub> towards photocatalytic degradation of MO and MB in water after 4 hours.	75
Table 5.5: Kinetic parameter of pseudo-first order and pseudo-second order kinetic model in MO dye.	79
Table 5.6: Kinetic parameter of pseudo-first order and pseudo-second order kinetic model in MB dye.	81

## LIST OF FIGURES

	Page
Figure 2.1: Characteristics of hydroxyl radical.	9
Figure 2.2: A photocatalytic mechanism during irradiation of UV light.	12
Figure 2.3: Titanium dioxide powder.	13
Figure 2.4: Crystalline structures of titanium dioxide (a) anatase,	14
Figure 2.5: Various applications of TiO <sub>2</sub> photocatalysis in environment and energy fields.	18
Figure 2.6: Degrading process on self-cleaning surfaces.	19
Figure 2.7 : Decomposition of malodorous substances by photocatalytic air purifier.	21
Figure 2.8: Formation of a crystalline metal-organic framework from a combination of a metal ion with an organic linker.	22
Figure 2.9: Structural representations of several coordination geometries of metal nodes including (a) trigonal planar, (b) square planar, (c) tetrahedral and (d) tetragonal paddlewheel.	24
Figure 2.10: Examples of common organic linkers used in construction of MOFs.	25
Figure 2.11: Solvothermal synthesis of MOF structures.	26
Figure 2.12: Microwave-assisted synthesis of MOF structures.	27
Figure 2.13: Sonochemical synthesis of MOF structures.	28
Figure 2.14: Mechanochemical synthesis of MOF structures.	29
Figure 2.15: Potential application of MOFs.	30
Figure 2.16: Chemical structure of MIL-53(Fe).	31
Figure 2.17: Methyl orange.	34
Figure 2.18: Methylene blue.	35
Figure 3.1: Synthesis of MIL-53(Fe) through reflux method.	38
Figure 3.2: Schematic diagram of X-ray diffractometer.	41
Figure 3.3: Hitachi S-3400 N Scanning electron microscope.	42
Figure 3.4: Photoreactor setup.	44
Figure 4.1: Mixture solution colour at the (a) beginning (clear dark brown) and at the (b) end (light orange) of reflux process.	47
Figure 4.2: MIL-53(Fe) powder.	48

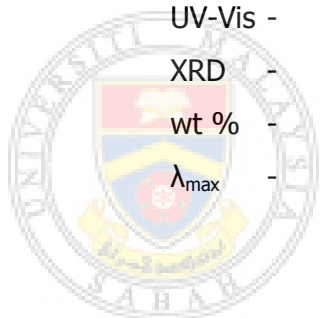
	Page
Figure 4.3: TiO <sub>2</sub> powder.	48
Figure 4.4: MIL-53(Fe)/TiO <sub>2</sub> at (a) 0.25% MIL-53(Fe); (b) 0.50% MIL-53(Fe); (c) 0.75% MIL-53(Fe) to TiO <sub>2</sub> ratio; and MIL-53(Fe) derived Fe <sub>2</sub> O <sub>3</sub> /TiO <sub>2</sub> at (d) 0.25% MIL-53(Fe); (e) 0.50% MIL-53(Fe); (f) 0.75% MIL-53(Fe) to TiO <sub>2</sub> ratio.	49
Figure 4.5: XRD pattern of MIL-53(Fe). Simulated MIL-53(Fe) for comparison from Du <i>et al.</i> , (2011).	50
Figure 4.6: XRD pattern of as-synthesized MIL-53(Fe), hydrothermally annealed TiO <sub>2</sub> , 0.25% MIL-53(Fe)/TiO <sub>2</sub> compared with XRD pattern of reference for anatase (Viswanathan & Raj, 2009).	51
Figure 4.7: XRD pattern of as-synthesized MIL-53(Fe), calcined TiO <sub>2</sub> , 0.75% MIL-53(Fe) derived Fe <sub>2</sub> O <sub>3</sub> /TiO <sub>2</sub> compared with XRD pattern of reference for anatase (Viswanathan and Raj, 2009).	52
Figure 4.8: EDX spectrum of as-synthesized MIL-53(Fe).	54
Figure 4.9: EDX spectrum of as-synthesized hydrothermally annealed TiO <sub>2</sub> .	55
Figure 4.10: EDX spectrum of as-synthesized hydrothermally annealed 0.25%MIL-53(Fe)/TiO <sub>2</sub> .	55
Figure 4.11: EDX spectrum of as-synthesized calcined TiO <sub>2</sub> .	56
Figure 4.12: EDX spectrum of as-synthesized calcined 0.75% MIL-53(Fe)/TiO <sub>2</sub> .	56
Figure 4.13: SEM micrographs of as-synthesized MIL-53(Fe).	58
Figure 4.14: SEM Micrograph of Hydrothermally Annealed TiO <sub>2</sub> under 20,000 magnifications.	58
Figure 4.15: SEM Micrograph of Hydrothermally Annealed 0.25% MIL-53(Fe)/TiO <sub>2</sub> under 25,000 magnifications.	59
Figure 4.16: SEM Micrograph of Calcined TiO <sub>2</sub> under 25,000 magnifications.	59
Figure 4.17: SEM Micrograph of Calcined 0.75% MIL-53(Fe)/TiO <sub>2</sub> under 20,000 magnifications.	60
Figure 5.1: Effect of MIL-53(Fe) to TiO <sub>2</sub> ratio of MIL-53(Fe)/TiO <sub>2</sub> in photocatalytic degradation of (a) MO and (b) MB in water over period of 6 hours.	62
Figure 5.2: Effect of MIL-53(Fe) to TiO <sub>2</sub> ratio synthesized of MIL-53(Fe) derived Fe <sub>2</sub> O <sub>3</sub> /TiO <sub>2</sub> by in photocatalytic degradation of (a) MO and (b) MB in water over a period of 6 hours.	64

Figure 5.3: Photocatalytic activity of different amount of 0.25% MIL-53(Fe) /TiO <sub>2</sub> towards (a) MO and (b) MB in water over a period of 6 hours.	67
Figure 5.4: Photocatalytic activity of different amount of 0.75% MIL- 53(Fe) derived Fe <sub>2</sub> O <sub>3</sub> /TiO <sub>2</sub> towards (a) MO and (b) MB in water over a period of 6 hours.	68
Figure 5.5: Photocatalytic activity of (a) 0.25% MIL-53(Fe)/TiO <sub>2</sub> and (b) 0.75% MIL-53(Fe) derived Fe <sub>2</sub> O <sub>3</sub> /TiO <sub>2</sub> towards MO and MB in water over a period of 6 hours.	71
Figure 5.6: Effect of H <sub>2</sub> O <sub>2</sub> in degradation of (a) MO and (b) MB in water by 0.100 g/L 0.25% MIL-53(Fe)/TiO <sub>2</sub> .	75
Figure 5.7: (a) Pseudo-first Order Kinetic and (b) Pseudo-second Order Kinetic of 0.25% MIL-53(Fe)/TiO <sub>2</sub> in 20 ppm MO solution.	78
Figure 5.8: (a) Pseudo-first order kinetic and (b) pseudo-second order kinetic of 0.25% MIL-53(Fe)/TiO <sub>2</sub> in 20 ppm MB solution.	80
Figure 5.9: schmematic diagram for the photocatalytic activity mechanism of MIL-53(Fe)/TiO <sub>2</sub> under UV-A Light irradiation.	82



## LIST OF SYMBOLS AND ABBREVIATIONS

AOP	-	Advance oxidation process
$D_{abs}$	-	Photodegradation efficiency
EDX	-	Energy-dispersive X-ray
eV	-	Electronvolt
$h^+$	-	Photogenerated holes
MB	-	Methylene blue
MIL	-	Materials of Institute Lavoisier
MO	-	Methyl orange
MOFs	-	Metal-organic frameworks
SEM	-	Scanning electron microscopy
TGA	-	Thermogravimetric analysis
UV-A	-	Ultraviolet A
UV-Vis	-	Ultraviolet-visible
XRD	-	X-ray diffractometer
wt %	-	Weight percentage
$\lambda_{max}$	-	Maximum wavelength



UMS  
UNIVERSITI MALAYSIA SABAH

## LIST OF APPENDICES

	Page
Appendix A Calculation of MIL-53(Fe) to TiO <sub>2</sub> Ratio	103
Appendix B Preparation of MO Dye Solution	104
Appendix C Preparation of MB Dye Solution	105
Appendix D Parameters for plotting first-order kinetics of Langmuir- Hinshelwood for photocatalytic degradation of MO dye.	106
Appendix E Parameters for plotting first-order kinetics of Langmuir-Hinshelwood for photocatalytic degradation of MB dye.	108
Appendix F Parameters for plotting second-order kinetics for photocatalytic degradation of MO dye.	110
Appendix G Parameters for plotting second-order kinetics for photocatalytic degradation of MB dye.	113



UMS  
UNIVERSITI MALAYSIA SABAH



# CHAPTER 1

## INTRODUCTION

### 1.1 Photocatalytic Degradation of Organic Pollutants by Titanium Dioxide

Photocatalytic degradation has been considered as an efficient way to solve the environmental pollution worldwide due to its ability to convert solar energy into chemical energy (Akple *et al.*, 2015; Xiang *et al.*, 2015). In water treatment field, advanced oxidation processes (AOPs) were proven to be very effective for the degradation of organic pollutant in the wastewater (Arslan *et al.*, 1999; Bergamini *et al.*, 2009). AOP in wastewater treatment generates sufficient quantity of hydroxyl radicals ( $\bullet\text{OH}$ ) with very high oxidizing power which capable to degrade recalcitrant organic pollutants (Banerjee *et al.*, 2007; Da Silva *et al.*, 2011) to  $\text{CO}_2$  and  $\text{H}_2\text{O}$  (Rathi *et al.*, 2003). Moreover, the removal and degradation of pollutants are very difficult using conventional treatment methods. Conventional water treatment methods such as adsorption on activated carbon, coagulation, and membrane separation has several disadvantages such as high operating costs and generate secondary pollutants resulting from transferring pollutants towards a new medium process (Damardji *et al.*, 2009).

Photocatalyst such as  $\text{TiO}_2$  is one of the materials (Kangwansupamonkon *et al.*, 2010) which were mostly applied in AOPs process.  $\text{TiO}_2$  penetrated by UV light give rise to hydroxyl radicals ( $\bullet\text{OH}$ ) that is important for the degradation of organic pollutants. This process is called AOP. In AOP,  $\text{TiO}_2$  can be photo-excited by radiation with a wavelength below 380 nm producing positive hole ( $h^+$ ) at the valence band and electron at the conduction band of  $\text{TiO}_2$  which will then react with water molecules or hydroxide ions ( $\text{OH}^-$ ) to produce hydroxyl radical ( $\bullet\text{OH}$ ). The  $\bullet\text{OH}$  has high oxidizing properties that capable of degrading and eventually mineralizing organic contaminants into  $\text{CO}_2$  and  $\text{H}_2\text{O}$  (Rathi *et al.*, 2003).

Nowadays, modification of TiO<sub>2</sub> has been extensively investigated aiming for more unique properties and functionality of the photocatalyst. Various approaches have been implemented such as impurity doping, noble metal deposition, coupling with narrow gap materials and modification with nanostructures (Qi *et al.*, 2016). The main objectives of the TiO<sub>2</sub> modifications are to improve the charge carrier separation yielding more •OH species that enhance the photocatalytic performances and to overcome wide band gap of the photocatalyst (Qi *et al.*, 2016; Kumar and Rao, 2017).

Beside TiO<sub>2</sub>, other metal oxides photocatalyst such as ZnO and WO<sub>3</sub> are also studied and been modified due to their stability, non-toxicity, ease of preparation, biocompatibility and their structure-electronic properties. These metal oxides are widely applied in heterogeneous photocatalysis owing to their valence band (VB) ability to generate •OH radicals and their identical band gap excitation mechanism (Kumar and Rao, 2017). However, among these metal oxides photocatalyst, TiO<sub>2</sub> is proven to generate the highest amount of hydroxyl radicals and has the highest activity compared to other semiconductor photocatalyst which contribute to more efficient photocatalytic activity (Xiang *et al.*, 2011; Kumar and Devi, 2011).

## **1.2 Problems of TiO<sub>2</sub> as Photocatalyst**

TiO<sub>2</sub> is one of the most used semiconductor materials owing to its non-toxicity, chemical stability, inexpensive and high efficiency in photocatalysis applications. However, TiO<sub>2</sub> photocatalyst facing several problems that limit its photocatalytic performance such as rapid electron-hole recombination, fast desorption of organic pollutants which can slow down the photocatalytic degradation and wide band gap energy of 3.2 eV where ultraviolet (UV) light is needed as an excitation source (Ganesh *et al.*, 2012; Kokila *et al.*, 2011). However, the high recombination rate which limits its catalytic performance is the major problem.

Recombination of electron and holes takes place either on the surface or in the bulk of the TiO<sub>2</sub> which are caused by impurities or defects resulting in the imperfection of the crystals surface or bulk (Choi *et al.*, 1994; Serpone, 1997).

Once the recombination occur, the excited electron will return back to the valence band without reacting with the adsorbed species (Sclafani and Herrmann, 1996).

Thus, the design of highly efficient photocatalyst with the ability to decrease the recombination rate semiconductor along with high mobility of electron and hole including having a numerous active sites is focused in this research. The photocatalytic activity will increase accordingly as the density of the surface  $\bullet\text{OH}$  increases due to its high oxidizing power capable to degrade organic pollutants into harmless materials such as  $\text{CO}_2$  and  $\text{H}_2\text{O}$ . Sufficient amount of  $\bullet\text{OH}$  are crucial to enhance the photocatalytic degradation efficiency of the  $\text{TiO}_2$  (Banerjee *et al.*, 2007; Rathi *et al.*, 2003). Therefore, modifying the  $\text{TiO}_2$  surface is rationale to study the its effect and eventually increase the concentration of  $\bullet\text{OH}$  in enhancing the photocatalytic efficiency.

### **1.3 Modification of $\text{TiO}_2$ with Metal-Organic Frameworks (MOFs)**

Numerous study and efforts in modifying  $\text{TiO}_2$  photocatalyst has been devoted aiming to improve and overcome the critical problems of unmodified  $\text{TiO}_2$  such as fast electron hole recombination and low efficiency in visible light absorption (Nasirian and Mehrvar, 2016; Qi *et al.*, 2016). To date, there has been a growing number of publications on the modification of  $\text{TiO}_2$  photocatalyst such as integrating with metal and non metal, impurity doping, noble metal deposition, coupling with narrow gap materials and modification with nanostructures (Qi *et al.*, 2016; Kumar *et al.*, 2014; Sun *et al.*, 2013). In this research, we aim to enhance the photocatalytic property of  $\text{TiO}_2$  by reducing the electron-hole recombination and increasing the active sites of photocatalyst through incorporation of metal-organic frameworks.

Metal-organic frameworks (MOFs) are new generation of inorganic-organic porous solids. They are hybridized materials constructed by metal nodes coordinated with organic linkers as bridging molecules to give three-dimensional (3D) structures (Zhou *et al.*, 2012). The variability of organic and inorganic components, highly crystalline and porous properties makes MOFs as promising

materials for versatile applications such as energy storage, molecules adsorption and separation, catalysis and drugs delivery (Czaja *et al.*, 2009).

Due to the MOFs unique characteristics such as high surface areas ranging from 1000 to 10,000 m<sup>2</sup>/g and high adsorption affinities (for example by Zn-based metal-organic frameworks, TMU-5 and TMU-6 which adsorb 96.2% and 92.8% of 100 ppm rhodamine B dye respectively), it can be considered as a good support for materials with photocatalytic properties which favor the diffusion of foreign species from water (Li *et al.*, 2009; Furukawa *et al.*, 2013; Masoomi *et al.*, 2016). MOFs have been reported as potential photocatalysts for the photocatalytic degradation of organic pollutants (Wang *et al.*, 2014). Owing to the significant properties of MOFs such as high density of active sites and high tunable properties, MOFs can serve as the potential candidate in photocatalysis (Corma *et al.*, 2010; Stock and Biswas, 2012). The combination of MOFs and TiO<sub>2</sub> might therefore improve the performance of TiO<sub>2</sub> in photocatalysis.

MIL-53(Fe) is a subclass of MOFs which were built up from chains of Fe(III) octahedra and 1,4-benzenedicarboxylic acid. This iron-based MOF has been selected to be incorporated into TiO<sub>2</sub> since it contains high iron oxoclusters and has been proved to be effective for common application in both catalysis and photocatalysis process (Liang *et al.*, 2015; Wang and Wang, 2015; Sciortino, *et al.*, 2015). Apart from that, low recombination rate are expected due to the small size of the Fe(III)-oxide cluster thus contributes to the enhancement of the photocatalytic degradation efficiency (Liang *et al.*, 2015). Moreover, the MIL-53(Fe) consisting of Fe(III) as the metal nodes where the empty *d* orbitals will form conduction band when mix with the organic ligands. This property was similar to the TiO<sub>2</sub> where its conduction band was built by empty Ti 3*d* orbitals (Gascon *et al.*, 2008). It is believed that the incorporation of MIL-53(Fe) in TiO<sub>2</sub> through hydrothermal and calcinations which produce MIL-53(Fe)/TiO<sub>2</sub> and MIL-53(Fe) derived Fe<sub>2</sub>O<sub>3</sub>/TiO<sub>2</sub> respectively favours the appearance of many active sites for photocatalytic degradation.

## 1.4 Objectives

The objectives of this study are to:

- (i) Prepare and characterize MIL-53(Fe)/TiO<sub>2</sub> and MIL-53(Fe) derived Fe<sub>2</sub>O<sub>3</sub>/TiO<sub>2</sub> composite,
- (ii) Evaluate the photocatalytic activity of MIL-53(Fe)/TiO<sub>2</sub> and MIL-53(Fe) derived Fe<sub>2</sub>O<sub>3</sub>/TiO<sub>2</sub> towards the degradation methyl orange (MO) and methylene blue (MB) dye in water,
- (iii) Determine the reaction kinetics of the MIL-53(Fe)/TiO<sub>2</sub> photocatalyst towards MO and MB.
- (iv) Evaluate the effect of H<sub>2</sub>O<sub>2</sub> towards the reaction kinetics of the MIL-53(Fe)/TiO<sub>2</sub> photocatalyst towards MO and MB.

## 1.5 Scope of Study

MIL-53(Fe) powder was synthesized by solvothermal-reflux method reported by Munn *et al.* (2013) while TiO<sub>2</sub> was prepared under hydrothermal synthesis according to Yang *et al.*, (2015). The product were further used to synthesis MIL-53(Fe)/TiO<sub>2</sub> by hydrothermal annealing and MIL-53(Fe) derived Fe<sub>2</sub>O<sub>3</sub>/TiO<sub>2</sub> photocatalyst by calcination using furnace. In this study, the optimum conditions for preparing MIL-53(Fe)/TiO<sub>2</sub> composites/nanoparticles were investigated. Four parameters/conditions were optimized consisted of: (i) amount of MIL-53(Fe) incorporated into TiO<sub>2</sub>; (ii) effect of photocatalyst amount; (iii) effect towards the degradation of MO and MB dyes; (iv) effect of initial concentration of H<sub>2</sub>O<sub>2</sub> towards the photocatalytic degradation of MO and MB dyes. All the synthesized samples were then characterized by X-ray diffractometer (XRD) to confirm the crystal structure of the samples and energy dispersive x-ray spectroscopy (EDX) to provide the elemental concentrations in the samples. The morphology of all samples was observed under scanning electron microscope (SEM). The photocatalytic activity of photocatalysts MIL-53(Fe)/TiO<sub>2</sub>, MIL-53(Fe) derived Fe<sub>2</sub>O<sub>3</sub>/TiO<sub>2</sub> and a control sample of TiO<sub>2</sub> were evaluated towards the degradation of methyl orange (MO) and

methylene blue (MB) dyes in aqueous solution under UV-vis light irradiation at different time interval. Due to their toxicity, it is very crucial to remove them from water. For that reason, throughout this research, MO and MB were selected as the representative acidic (anionic) dye and basic (cationic) dye respectively. The absorbances were recorded by ultraviolet-visible (UV-Vis) spectroscopy. Langmuir-Hinshelwood model and pseudo-second order were studied for the degradation kinetics of the photocatalysts.



UMS  
UNIVERSITI MALAYSIA SABAH

## CHAPTER 2

### LITERATURE REVIEW

#### 2.1 Advanced Oxidation Processes (AOP)

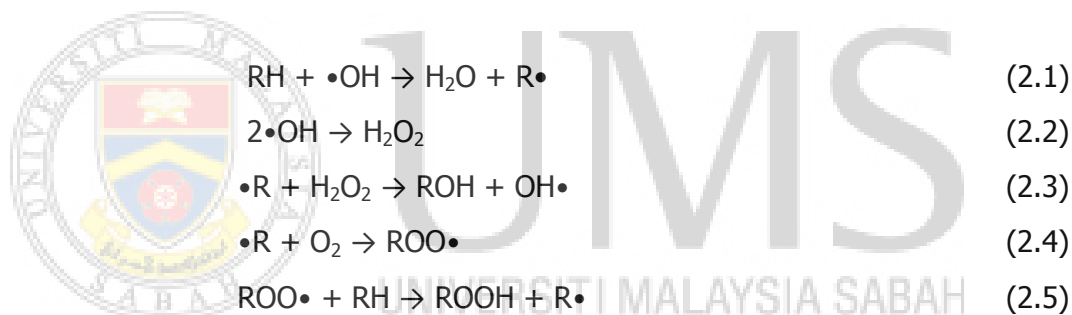
Oxidation is a chemical reaction which involves the transfer of one or more electrons from an electron donor to an electron acceptor. A chemical transformation of both the oxidant and reactant occurred due to the electron transfer process which in some cases producing chemical species with an odd number of valence electrons known as radicals. Radical species is an unpaired electron which is highly unstable and reactive. It will undergo additional oxidation with organic or inorganic reactants to form stable oxidation products (Carey, 1992).

Over the past three decades, advanced oxidation processes (AOPs) have earned a significant level of interest for the treatment of drinking water and wastewater industry. Advanced oxidation processes (AOPs) are technologies which involved the generation of highly reactive and non-selective oxidant, hydroxyl radicals, primarily used to destroy a wide range of toxic organic compound that cannot be oxidized by conventional oxidant present in wastewater, soil and air (Glaze *et al.*, 1987). The toxic pollutants will eventually oxidized into mineral end-products which will yield CO<sub>2</sub> and inorganic ions. Table 2.1 shows the comparison of relative oxidation power of several oxidizing species. Hydroxyl radicals which are one of the strongest oxidants in an aqueous medium able to oxidize a wide range of recalcitrant pollutants into harmless compound such as mineral salts, carbon dioxide and water through mineralization process (Chen *et al.*, 2000). Figure 2.1 shows some interesting characteristics of hydroxyl radical that brings AOPs as a powerful chemical treatment procedure to remove organic contaminants. A common reaction for the initial attack once the hydroxyl radicals generated is the abstraction of hydrogen atom from water to initiate a radical chain oxidation (Munter, 2001). The reactions were shown in Equation 2.1 to 2.5.

**Table 2.1: Comparison of relative oxidation power of some oxidizing species**

Oxidizing species	Relative oxidation power
Chlorine, $\text{Cl}_2$	1.00
Hypochlorous acid, HOCL	1.10
Permanganate, $\text{MnO}_4$	1.24
Hydrogen peroxide, $\text{H}_2\text{O}_2$	1.31
Ozone, $\text{O}_3$	1.52
Atomic oxygen, O	1.78
Hydroxyl radical ( $\bullet\text{OH}$ )	2.05
Fluorine, $\text{F}_2$	2.25
Positively-charged hole on titanium dioxide, $\text{TiO}_2^+$	2.35

Source: Carey (1992); Zhou and Smith (2002)



AOP can be classified into two classes which are homogeneous and heterogeneous (Huang *et al.*, 1993). Table 2.2 shows a classification of AOP. Heterogeneous photocatalysis applying the usage of semiconductor such as zinc oxide ( $\text{ZnO}$ ), tin dioxide ( $\text{SnO}_2$ ) and  $\text{TiO}_2$  in the presence of UV irradiation and hydrogen peroxide ( $\text{H}_2\text{O}_2$ ). The main advantages of these methods are high rates of pollutant oxidation, flexibility concerning water quality variations, and small dimension of the equipment.